PROCEEDINGS OF SCIENCE

GROND coverage of the main peak of GRB 130925A

Jochen Greiner[*†]
Max-Planck-Institut für extraterrestrische Physik, 85748 Garching, Germany
E-mail: jcg@mpe.mpg.de

H.-F. Yu[1], **T. Krühler**[2], **D. D. Frederiks**[3], **A. Beloborodov**[4], **P. N. Bhat**[5], **J. Bolmer**[6,1], **H. van Eerten**[1], **R. L. Aptekar**[3], **J. Elliott**[1], **S. V. Golenetskii**[3], **J. F. Graham**[1], **K. Hurley**[7], **D. A. Kann**[8], **S. Klose**[8], **A. Nicuesa Guelbenzu**[8], **A. Rau**[1], **P. Schady**[1], **S. Schmidl**[8], **V. Sudilovsky**[1], **D. S. Svinkin**[3], **M. Tanga**[1], **M. V. Ulanov**[3], **K. Varela**[1], **A. von Kienlin**[1], **X.-L. Zhang**[1]

[1] *Max-Planck-Institut für extraterrestrische Physik, 85748 Garching, Germany*
[2] *European Southern Observatory, Santiago 19, Chile*
[3] *Ioffe Physical-Technical Institute, St. Petersburg, 194021 Russia*
[4] *Columbia University, Physics Dept., 538 W 120th Street, New York, NY 10027, U.S.A.*
[5] *Center for Space Plasma and Aeronomic Res., Univ. Alabama, Huntsville AL 35805, U.S.A.*
[6] *Technische Universität München, Physik Dept., 85748 Garching, Germany*
[7] *Space Sciences Laboratory, University of California, Berkeley, CA 94720, U.S.A.*
[8] *Thüringer Landessternwarte Tautenburg, 07778 Tautenburg, Germany*

We performed dedicated observations of the ultra-long duration (T90 about 7000 s) GRB 130925A in the optical/near-infrared with the 7-channel "Gamma-Ray Burst Optical and Near-infrared Detector" (GROND) at the 2.2m MPG/ESO telescope. We detect an optical/NIR flare with an amplitude of nearly 2 mag which is delayed with respect to the keV–MeV prompt emission by about 300–400 s. The decay time of this flare is shorter than the duration of the flare (500 s) or its delay. While we cannot offer a straightforward explanation, we discuss the implications of the flare properties and suggest ways toward a possible interpretation.

Swift: 10 Years of Discovery,
2-5 December 2014
La Sapienza University, Rome, Italy

[*]Speaker.
[†]Based on the full paper published in A&A 568 (2014) A75

PoS(SWIFT 10)010

1. Introduction

GRB 130925A triggered the Gamma-Ray Burst Monitor (GBM, Meegan et al. 2008) on the *Fermi* satellite first at 03:56 UT on 25 September 2013 on what seems to be a precursor, and a second time at 04:09 UT [10]. Subsequently, the Burst Alert Telescope (BAT) on the *Swift* satellite [11] triggered at T_0(BAT) = 04:11:25 UT = 15085 s (trigger=571830; [21]). Also, INTEGRAL SPI/ACS [25] and MAXI/GSC [28] triggered on this gamma-ray burst, and Konus-Wind detected it in waiting mode [12]. The *Swift* XRT and UVOT observations started at 147 s after the trigger. A bright X-ray source was found at RA (2000.0) = $02^{\rm h}44^{\rm m}42\overset{\rm s}{.}4$, Decl. (2000.0) = $-26^\circ09'16''$ with an error radius of $5\overset{''}{.}1$ [21]. UVOT did not detect any obvious emission, but with GROND a very red source was detected [26]. Subsequent spectroscopy with UVES [30] and X-Shooter [27] revealed multiple emission lines, suggestive of a host galaxy redshift of z=0.347.

Here, we describe our GROND observations of the second gamma-ray emission peak as observed by Konus-Wind and INTEGRAL SPI/ACS.

2. Observations

2.1 Konus-Wind data

GRB 130925A was observed as a count rate increase in the S1 detector. Thanks to the remote KW orbit around the Lagrangian point L1, with stable background and lack of Earth or planet occultations, the instrument was able to measure the burst's prompt emission for more than 5000 s.

Konus-Wind did not trigger on any of the various peaks. Thus, count rates with a coarse time resolution of 2.944 s are recorded in three energy bands: G1 (26–99 keV), G2 (99–394 keV), and G3 (394–1480 keV). The time history recorded in the three Konus-Wind energy bands can be considered as a continuous three-channel spectrum covering the 26–1480 keV energy range. After subtracting the background emission as estimated by a polynomial fit from before the precursor to well after the third emission period, we measure the following fluences (all in the standard KW 20–10000 keV band) for the different emission episodes based on cut-off powerlaw fits to the spectra: 1st major episode (14961–15264 s UT) : $9.5\pm0.7\times10^{-5}$ erg cm^{-2}; 2nd major episode (16766–17964 s UT) : $3.9\pm0.1\times10^{-4}$ erg cm^{-2}; 3rd major episode (18768–19463 s UT) : $5.6\pm0.9\times10^{-5}$ erg cm^{-2}. The total fluence, which accounts also for the weaker inter-pulse emission, is $6.2\pm0.3\times10^{-4}$ erg cm^{-2} ($2.9\pm0.2\times10^{52}$ erg for the first emission episode; $1.2\pm0.04\times10^{53}$ erg for the second). At $z = 0.347$ and standard cosmology ($H_{\rm o}$=70 km/s/Mpc, $\Omega_{\rm M}$=0.27, Ω_Λ=0.73), this implies an isotropic equivalent energy release of $E_{\rm iso}$ = $1.9\pm0.1\times10^{53}$ erg. This is one of the most energetic low-redshift GRBs.

2.2 INTEGRAL SPI/ACS data

The SPI-ACS data were taken from the Integral Data Centre. The original 50 ms, 0.1–10 MeV light curve was rebinned into 8 s temporal bins, but analyzed at their finest time resolution for the minimum variability timescale.

2.3 GROND and VLT observations

GROND [13] exposures automatically started 350 s after the arrival of the *Swift*/BAT trigger. Simultaneous imaging in $g'r'i'z'JHK_s$ continued for nearly 6 hrs, with the last exposures done only in the NIR channels due to morning twilight (after 09:36 UT). Further observations were done in the mornings of Sep 26, 27 and 29, with one late-time deep host imaging on Oct. 6. GROND data have been reduced in the standard manner [18] using pyraf/IRAF [29, 19]. The optical/NIR imaging was calibrated against the primary SDSS[1] standard star network, or catalogued magnitudes of field stars from the SDSS in the case of $g'r'i'z'$ observations, or the 2MASS catalog for JHK_s imaging. This results in typical absolute accuracies of ± 0.03 mag in $g'r'i'z'$ and ± 0.05 mag in JHK_s.

We find a variable optical/NIR object at position RA(2000.0) = 02:44:42.96, Decl.(2000.0)= –26:09:11.2 ($\pm 0\farcs3$) which is fully consistent with the *Swift*/XRT $1\farcs4$ error circle (*Swift*/XRT repository). We therefore identify this object as the optical/NIR counterpart of GRB 130925A; its light curve in all 7 GROND filters is shown in Fig. 1.

In order to more accurately estimate the contribution of the constant host flux to the early- and late-time light curve, we observed the field of GRB 130925A with the ESO/VLT UT4 equipped with HAWK-I. Observations started on October 13, 2013, 06:21 UT, which is 18.1 days after the GRB trigger. They were performed under clear sky conditions and consist of sets of dithered exposures with a total integration time of 30, 12, 10 and 16 minutes in the Y, J, H and K_s filter respectively. Data reduction and photometric calibration was performed in a similar fashion as for the GROND data. The measurements are shown as the temporally last data points in Fig. 1.

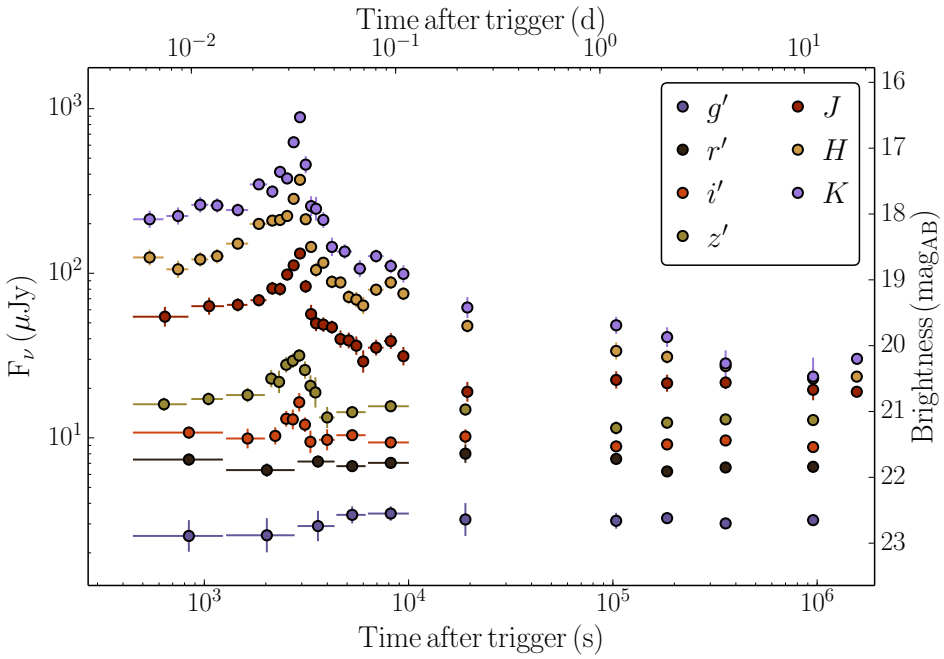

Figure 1: Light curve of the afterglow of GRB 130925A in the 7 GROND filters. The times are relative to the *Swift*/BAT trigger time. The very last epoch measurements are from HAWK-I observations and represent our best estimate of the host magnitudes.

[1] http://www.sdss.org

2.4 Swift data

Swift/BAT triggered on the first emission episode (not on the precursor which triggered GBM), and follow-up observations with the XRT and UVOT instruments started about 150 s after the BAT trigger [21]. While a thorough analysis of all the *Swift* data has appeared already [9], we use some *Swift*/XRT observations to compare with the GROND data. The corresponding data have been extracted from the *Swift*/XRT repository [8].

3. Results

3.1 Minimum variability time scale of the prompt emission

The variability in the γ-ray light curve of GRBs is, in most models, related to a physical origin in the central engine, likely convolved with the bulk Lorentz factor of the outflow. We have estimated the minimum variability time scale (MVT) in GRB 130925A with the new method recently developed for high time-resolution GBM data [4]. For the precursor and the first and the third peak as seen by *Fermi*/GBM, we derive the following MVT: 0.39±0.02 s, 0.92±0.01 s, 6.7±2.2 s, respectively. For the INTEGRAL/ACS, we obtain 1.10±0.19 s, 4.82±1.86 s and 14.2±5.2 s for the first, second and third peak, respectively. This shows the typical behaviour of increasing MVT with time. Given that the INTEGRAL/ACS and *Fermi*/GBM data show good consistency for the first and third peaks, we can be confident in the INTEGRAL-derived MVT value for the second peak, where we have no GBM coverage. [4] has estimated the mean MVT for short- and long-duration GRBs as 0.024 s and 0.25 s, respectively (see his Fig. 3). Thus, the MVT of about 1 s for the first and about 5 s for the second peak of GRB 130925A falls in the longest 5%/1% percentile of the distribution of long-duration GRBs.

If the MVT relates to the bulk Lorentz factor, then GRB 130925A might feature one of the lowest Lorentz factors encountered so far. Applying the formalism of [22], and carrying forward the error of the spectral slope to estimate the flux at 1 MeV, we obtain minimum Lorentz factors of 37, 20 and 31 for the precursor, first and third peak. We note, though, that using e.g., the Γ_o-$E_{\gamma,iso}$ relation of [20], we obtain values up to a factor 10 higher.

3.2 A normal optical/NIR/X-ray afterglow?

For a combined Swift/XRT and GROND SED we have selected time intervals for both instruments which were not affected by flares, and performed a simultaneous spectral fit. Since the X-ray spectral slope is substantially steeper than the extinction-corrected optical/NIR slope, we employ a broken power law. In contrast to the typical GRB afterglow SEDs [e.g., 14] a fit with a fixed slope difference of 0.5 between the optical/NIR and X-ray part is rejected at high confidence. Fixing the redshift and the galactic foreground absorption of $N_H^{Gal} = 1.66 \times 10^{20}$ cm^{-2} [15] we obtain the following best-fit parameters: $N_H^{Host} = (1.5 \pm 0.1) \times 10^{22}$ cm^{-2}, $\beta_{opt/NIR} = 0.32 \pm 0.03$, $\beta_X = 1.6 \pm 0.1$, $E_{break} = 1.68 \pm 0.09$ keV, and $E(B-V) = 2.24 \pm 0.26$ mag for SMC-like dust, at a reduced χ^2=0.87 for 84 degrees of freedom. While formally an acceptable fit, this is incompatible on physical grounds with any previous afterglow modelling, and supports earlier conclusions that suggested a different origin of the X-ray emission, i.e., as dust-scattered prompt flux [9] or thermal emission from a hot cocoon [24].

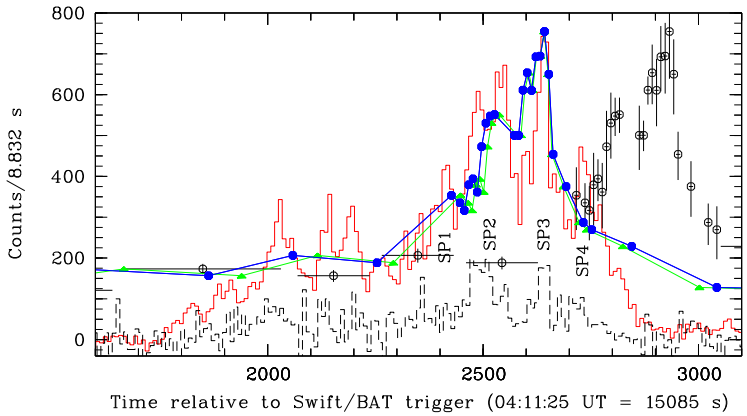

Figure 2: Expanded view of the delay of the GROND K_s-band light curve (open black symbols with error bars) with respect to the KW light curve (red line). In blue and green we show the shifted (-290 s) and stretched (time axis divided by 1.11) GROND K_s-band light curve, respectively. The black dashed curve at the bottom is the KW highest energy channel G3 (at a factor 3 stretched intensity scaling).

3.3 The delayed optical/NIR peak wrt. gamma-rays

Temporal properties: We see a very sudden increase in optical/NIR brightness at around 2.5 ks after the BAT trigger, followed by a rapid decline at 3 ks, followed by a more gentle decline beyond about 4 ks. There is a pronounced dip around 6 ks with another emission peak at 8 ks. Fitting a two-component model with a triangular-shaped flare on top of a gentle, smoothly-broken powerlaw (as used above) for the times before and well after the flare we derive a rise slope of $t^{+2.0\pm0.3}$ and a decay slope of $t^{-6\pm1}$, assuming a T_o at the beginning of the second gamma-ray pulse.

The most intriguing feature of GRB 130925A is the long delay (Fig. 2) of the optical/NIR emission peak relative to the γ-ray emission (second episode). Such lags have been seen in previous GRBs, though the present delay is surprisingly long: of 3040$\pm$30 s relative to the maximum of the first and 405$\pm$30 s relative to the maximum of the second gamma-ray episode.

When split into single 10 s integrations around the peak in the K_s/H-bands, we find some substructure (Fig. 2). To some extent, this substructure reflects the sub-pulse structure in the KW light curve, in particular the first three sub-pulses (SP1–SP3 in Fig. 2), though other features are missing or are less pronounced. A simple shift of the GROND K_s-band light curve (blue line in Fig. 2) is a better match than a time-stretch (green line). We also note that the best-fit shift in Fig. 2 is by –290 s, thus matching the peak of the K_s-band light curve with the sharp spike SP3, while the above mentioned shift of 405$\pm$30 s matches the highest fluence peak SP2. It is worth noting that the flare decay time of $\sim$20 s is much shorter than both the flare duration ($\sim$500 s) and its delay after the second peak ($\sim$300–400 s). The implications of this are discussed further below.

Combined GROND and Konus-Wind spectral fitting: We defined 11 time slices and performed a combined fit of the 3-channel KW spectra and the 3–5 (depending on significant excess emission above the host galaxy) filter GROND SED by employing a Band function [1]. Fixing the redshift, and requiring the same extinction in all 11 fits, we find that the fits are statistically acceptable (reduced χ^2=34.1/34 for 79 bins and 34 dof), but the resulting parameters are physically questionable. With a few exceptions, $E_{\rm peak}$ is always at the low-energy boundary of the G2 channel. Thus, we do not interpret this as evidence that the optical/NIR emission tracks the γ-ray emission.

4. Discussion

The data suggest two possible alternative interpretations. In the first, one would argue that the optical/NIR flare has occurred between the second and third gamma-ray emission episodes, and thus is part of the prompt emission, similar to the two X-ray flares before the optical/NIR flare. In this interpretation, one would need to explain why the spectral peak of the various emission episodes changes so drastically between gamma-rays and optical. In a second interpretation, one could consider the optical/NIR flare as delayed emission with respect to the second gamma-ray episode, in which case the challenge is to explain both the delay as well as the fast decay time. We discuss each of these options below.

4.1 The optical/NIR flare as part of the prompt emission

Hard-to-soft evolution: Analysis of energy-resolved gamma-ray light curves typically shows a generic hard-to-soft evolution of peaks throughout a GRB, manifesting in different features: (i) later peaks have smaller peak energies, (ii) soft energies lag hard energies [6, 23], (iii) the duration T_{90} gets larger with energy according to $E^{-0.4}$ [5]. In the case of GRB 130925A, the optical/NIR peak shows a delay which is consistent with a $E^{-0.4}$ dependence, but the widths of the peaks (or T_{90}) certainly do not. Thus, the observed optical/NIR peak is likely not a manifestation of the hard-to-soft evolution of GRB pulses, despite some similarity in the substructure of the emission.
A canonical flare: The optical/NIR flare seen with GROND is very unlikely to be the optical "counterpart" of a missed X-ray flare, because the times of three X-ray flares seen at 1,2 ks, 5 ks and 7 ks are covered by GROND data, and show no sign of flux enhancement. Also, the rise and decay times are different, namely $\sim$500 s in X-rays as compared to 20–30 s in the optical/NIR.
Reverse shock: The reverse shock is predicted to happen with little delay with respect to the gamma-ray emission unless the Lorentz factor is very small. The corresponding optical emission has a rise time power law index of +0.5 for both a wind and constant density profile, and a decay time power law index of about –2 for a constant density environment, or up to –3.0 for a wind density profile [16, 17]. The decay slopes are clearly inconsistent with our observations. The rise slope could be consistent with the self-absorbed case, but we observe a very sharp peak, so there is no flattening towards a non-self-absorbed phase with a +0.5 rise. We therefore exclude a reverse shock interpretation of the optical/NIR flare.

4.2 The optical/NIR flare as delayed emission

Dust destruction: A number of suggestions have been made in the past which relate the delayed onset of optical/UV emission to the effect of dust in the nearby surrounding medium. One scenario invokes a dense region around the GRB progenitor, similar to that of a molecular cloud. While the prompt gamma-rays and the X-ray afterglow would pass relatively unaffected, the optical emission would only pass once the dust along our line of sight is completely destroyed through thermal sublimation [e.g. 7]. In the case of GRB 130925A, this scenario is ruled out, because we observe no reduction of the best-fit extinction throughout the burst, to a limit of $\Delta A_{\rm V} < 0.4$ mag.
Pair-loaded fireball: A more promising possibility seems to be the framework of the $e^{\pm}$ enrichment originally proposed to explain the delayed GeV flash in *Fermi*/LAT data [3]. The prompt MeV radiation streaming ahead of the blast wave creates a large enrichment in $e^{\pm}$ which in turn

leads to substantial inverse Compton scattering of the prompt MeV photons, thus creating a GeV flash. This GeV emission starts while the prompt emission is still ongoing, but lasts longer because of a broader angular distribution of scattered photons. the delay of which relative to the GeV emission is determined by two parameters, the pair-loading radius and the Lorentz factor [3]. The pair-loading radius is $R_{\rm load} \approx 10^{17} E_{54}^{1/2}$ cm, where E_{54} is the isotropic equivalent energy of the prompt GRB energy ahead of the forward shock. For GRB 130925A, we take E_{54} as the sum of the first prompt pulse and half of the second, i.e. $E_{54} = 0.08$, and thus $R_{\rm load} = 2.9 \times 10^{16}$ cm. Together with the delay of 3040 / 405 s (relative to first or second episode) we obtain an inferred Lorentz factor of $\Gamma_{405s} \approx ((1+z) * R_{\rm load}/2c\delta t)^{1/2} \sim 40$ or $\Gamma_{3040s} = 11$.

In any case, the inferred Lorentz factors are of the same order of magnitude as the Lorentz factor derived above from the rising part of the afterglow, and the low absolute value of the inferred Lorentz factor is also nicely compatible with the exceptionally long minimum variability time scale.

The only potential mismatch with this pair-loaded fireball scenario is the sub-structure in the flare, as well as its fast decay time scale. It remains to be seen through detailed simulations whether this scenario will work for GRB 130925A.

Internal dissipation: Finally, the fast decay of the optical/NIR flare could be considered as evidence for an internal origin within the jet, similar to models for the X-ray flares (but see above section 4.1.). In the standard picture of the blast-wave emission the curvature effect implies that the decay time scale of a flare is of the same order of magnitude as its duration. This can be avoided either by a jet opening angle smaller than $1/\Gamma$, or by non-isotropic emission in the blast-wave frame [e.g., limb-brightened 2]. The former case is unlikely, as this GRB shows neither a particularly spiky light curve, nor evidence of particularly high Lorentz factor. In contrast, the latter case in fact also produces a delay of the emission at very small spreading in time, exactly as we observe in GRB 130925A. If this is the true interpretation, GRB 130925A might be the first observational evidence for limb-brightened jet emission.

If the optical/NIR flare and the second gamma-ray peak are indeed related, e.g. by being different episodes of emission from the same shell but at different radii, one would expect the GROND light curve to be stretched rather than only shifted with respect to the second gamma-ray peak (as Fig. 2 demonstrates, both options are consistent with the data, with a preference for a shift). The similarities between the two peaks are then likely the result of the imprint of the outflow geometry or jet structure on the emission, which might be dominated by different processes at the different frequencies.

5. Conclusions

We have observed a pronounced optical/NIR flare related to GRB 130925A. Our well-sampled multi-color GROND light curve shows a peak which is delayed by 290 s with respect to the second γ-ray peak. This is not dissimilar to several other GRBs for which prompt optical emission has been detected. However, the exquisite data quality for GRB 130925A allows us to exclude the leading contenders. First, given the delay by nearly the full pulse-width, the optical/NIR emission cannot be just the extrapolation of a Band (or any other broad-band) model extension from the γ-ray emission. Second, the typical interpretation of being due to a reverse shock also does not apply, since the optical/NIR peak in GRB 130925A exhibits a very sharp rise and an extremely

steep decay, both much faster than expected for a reverse shock. Other options have been discussed as well, suggesting that the main observational feature of the decay time being shorter than the delay time can, in principle, be explained. However, much more detailed considerations are needed to derive a coherent picture, which are beyond the scope of this paper.

Acknowledgements: JG and HFY acknowledge support by the DFG cluster of excellence "Origin and Structure of the Universe" (www.universe-cluster.de). PS, JFG and MT acknowledge support through the Sofja Kovalevskaja award to P. Schady from the Alexander von Humboldt Foundation Germany. SK and ANG acknowledge support by DFG grant Kl 766/16-1. SS acknowledges support by the Thüringer Ministerium für Bildung, Wissenschaft und Kultur, FKZ 12010-514. DAK acknowledges TLS Tautenburg for financial support. AvK and XLZ acknowledge support by DLR through funding by the BMWT under FKZ 50 OG 1101. KH is grateful for support under NASA grants NNX13AI54G, NNX11AP96G, and NNX07AR71G. Part of the funding for GROND (both hardware as well as personnel) was generously granted from the Leibniz-Prize to Prof. G. Hasinger (DFG grant HA 1850/28-1). The Konus-*WIND* experiment is partially supported by a Russian Space Agency contract, RFBR grants 15-02-00532 and 13-02-12017 ofi-m. This work made use of data supplied by the UK *Swift* Science Data Centre at the University of Leicester.

References

[1] Band D., Matteson J., Ford L. et al. *BATSE observations of gamma-ray burst spectra. I - Spectral diversity*, *ApJ* **413** (1993) 281
[2] Beloborodov A.M., Daigne F., Mochkovitch R., Uhm Z.L., *Is gamma-ray burst afterglow emission intrinsically anisotropic?*, *MNRAS* **410** (2011) 2422
[3] Beloborodov A.M., Hasoët R., Vurm I., *On the Origin of GeV Emission in Gamma-Ray Bursts*, *ApJ* **788** (2014) 36
[4] Bhat P.N., 2013,*Variability Time Scales of Long and Short GRBs* in proceedings of *7th Huntsville Gamma-Ray Burst Symposium, GRB 2013*, (2013)
[5] Bissaldi E., von Kienlin A., Kouveliotou C. et al., *First-year Results of Broadband Spectroscopy of the Brightest Fermi-GBM Gamma-Ray Bursts*, *ApJ* **733** (2011) 97
[6] Cheng L.X., Ma Y.Q., Cheng K.S., Zhou Y.Y., *The time delay of gamma-ray bursts in the soft energy band.*, *A&A* **300** (1995) 746
[7] Cui X.-H., Li Z., Xin L.-P., *Delayed onset and fast rise of prompt optical-UV emission from gamma-ray bursts in molecular clouds*, *Res. in Astron. Astrophys.* **13** (2013) 57
[8] Evans, P.A., Beardmore, A.P., Page, K.L., et al., *Methods and results of an automatic analysis of a complete sample of Swift-XRT observations of GRBs*, *MNRAS* **397** (2009) 1177
[9] Evans P.A., Willingale R., Osborne J.P. et al., *GRB 130925A: an ultralong gamma ray burst with a dust-echo afterglow, and implications for the origin of the ultralong GRBs*, *MNRAS* **444** (2014) 250
[10] Fitzpatrick G., *Fermi GBM detection of GRB 130925A and a possible precursor*, *GCN Circulars* (2013) 15255
[11] Gehrels N., Chincarini G., Giommi P., et al., *The Swift Gamma-Ray Burst Mission*, *ApJ* **611** (2004) 1005
[12] Golenetskii S., Aptekar R., Frederiks D. et al., *Konus-wind observation of GRB 130925A*, *GCN Circulars* (2013) 15260
[13] Greiner J., Bornemann W., Clemens C., et al., *GROND a 7-Channel Imager PASP* **120** (2008) 405
[14] Greiner J., Krühler T., Klose S. et al., *The nature of "dark" gamma-ray bursts*, *A&A* **526** (2011) A30
[15] Kalberla, P.M.W., Burton, W.B., Hartmann, D., et al., *The Leiden/Argentine/Bonn (LAB) Survey of Galactic HI. Final data release of the combined LDS and IAR surveys with improved stray-radiation corrections*, *A&A* **440** (2005) 775
[16] Kobayashi S., *Light Curves of Gamma-Ray Burst Optical Flashes*, *ApJ* **545** (2000) 807

[17] Kobayashi S., Zhang B., *Early Optical Afterglows from Wind-Type Gamma-Ray Bursts*, *ApJ* **597** (2003) 455
[18] Krühler T., Küpcü Yoldaş A., Greiner J. et al., *The 2175 Å Dust Feature in a Gamma-Ray Burst Afterglow at Redshift 2.45*, *ApJ* **685** (2008) 376
[19] Küpcü Yoldaş A., Krühler T., Greiner J., et al., *First Results of GROND AIP Conf. Proc.* **1000** (2008b) 227
[20] Liang E.-W., Yi S.-Y., Zhang J. et al., *Constraining Gamma-ray Burst Initial Lorentz Factor with the Afterglow Onset Feature and Discovery of a Tight* $\Gamma_0 - E_{gamma,iso}$ *Correlation*, *ApJ* **725** (2010) 2209
[21] Lien A.Y., Markwardt C.B., Page K.L. et al., *GRB 130925A: Swift detection of a burst*, *GCN Circulars* (2013) 15246
[22] Lithwick Y. & Sari R., *Lower Limits on Lorentz Factors in Gamma-Ray Bursts*, *ApJ* **555** (2001) 540
[23] Norris J.P., Marani G.F., Bonnell J.T., *Connection between Energy-dependent Lags and Peak Luminosity in Gamma-Ray Bursts ApJ* **534** (2000) 248
[24] Piro L., Troja E., Gendre B., et al., *A Hot Cocoon in the Ultralong GRB 130925A: Hints of a POPIII-like Progenitor in a Low-Density Wind Environment*, *ApJ* **790** (2014) 15
[25] Savchenko V., Beckmann V., Ferrigno C., et al., *Observation of possible GRB/TDE 130925A by INTEGRAL/SPI-ACS: three activity episodes*, lemphGCN Circulars (2013) 15259
[26] Sudilovsky V., Kann D.A., Greiner J., *GRB 130925A: GROND afterglow candidate*, *GCN Circulars* (2013a) 15247
[27] Sudilovsky V., Kann D.A., Schady P., Klose S., Greiner J., Krühler T., *GRB 130925A: VLT/X-shooter redshift*, *GCN Circulars* (2013b) 15250
[28] Suzuki K., Sakakibara H., Negoro H., et al., *GRB 130925A: MAXI/GSC detection*, *GCN Circulars* (2013) 15248
[29] Tody D., *IRAF in the Nineties*, in *ASP Conf. 52, Astronomical Data Analysis Software and Systems II, ed. R.J. Hanisch, R.J.V. Brissenden, & J. Barnes* (1993) 173
[30] Vreeswijk P.M., Malesani D., Fynbo J.P.U., De Cia A., Ledoux C., *GRB 130925A: VLT/UVES observations*, *GCN Circulars* (2013) 15249